Journal of Magnetism and Magnetic Materials 418 (2016) 236–241

Contents lists available at ScienceDirect

Journal of Magnetism and Magnetic Materials

journal homepage: www.elsevier.com/locate/jmmm

Effect of Co content on structure and magnetic behaviors of high induction Fe-based amorphous alloys

Rajat K. Roy*, Ashis K. Panda, Amitava Mitra

NDE & Magnetic Materials Group, MST Division, CSIR-National Metallurgical Laboratory, Jamshedpur 831007, India

ARTICLE INFO

Article history:
Received 30 November 2015
Received in revised form
8 February 2016
Accepted 18 February 2016
Available online 19 February 2016

Keywords:
Saturation magnetization
Coercivity
High temperature
Nanocrystallinity
Curie temperature

ABSTRACT

The replacement of Fe with Co is investigated in the $(Fe_{1-x}Co_x)_{79}Si_{8.5}B_{8.5}Nb_3Cu_1$ ($x=0$, 0.05, 0.2, 0.35, 0.5) amorphous alloys. The alloys are synthesized in the forms of ribbons by single roller melt spinning technique, and the structural and magnetic properties of annealed ribbons are characterized by X-ray diffraction (XRD), transmission electron microscopy (TEM) and vibrating sample magnetometer (VSM), *B–H* curve tracer, respectively. All as-cast alloys are structurally amorphous, however, their magnetic properties are varying with Co addition. The Co addition within 5–20 at% results in moderate thermal stability, saturation induction, Curie temperature and lowest coercivity, while 35 at% Co causes highest saturation induction, coercivity, Curie temperature and lowest thermal stability. On devitrification, the magnetic properties change with the generation of α-FeCo nanocrystallites and $(FeCo)_{23}B_6$, Fe_2B phases during primary and secondary crystallization stages, respectively. A small amount Co is advantageous for maintaining finer nanocrystallites in amorphous matrix even after annealing at 600 °C, leading to high saturation magnetization (> 1.5 T) and low coercivity (~ 35 A/m). The improved magnetic properties at elevated temperatures indicate these alloys have a potential for high frequency transformer core applications.

1. Introduction

The Fe and FeCo based amorphous alloys, specifically FINEMET and HITPERM, are promising materials in transformer industries owing to its superior soft magnetic properties and saturation magnetization, respectively. The enhancement of saturation magnetization as well as soft magnetic properties at elevated temperatures has always a great interest due to the increasing demand of high temperature applications of these materials [1]. In FINEMET (Fe–Si–B–Nb–Cu) type alloys, the soft magnetic properties are superior owing to good glass forming ability and nanocrystallinity at the annealed state [2–4]. However, these alloys have poor saturation magnetization compared to silicon steel, limiting its industrial application. Although HITPERM (Fe–Co–M–B–Cu; M=Zr, Nb, Hf) and NANOPERM (Fe–M–B–Cu; M=Zr, Nb, Hf) alloys possess good saturation magnetization, but their soft magnetic properties are deteriorated [5–7]. Saturation magnetization and Curie temperature are the intrinsic magnetic properties, depending on alloy chemistry and crystal structure, where as soft magnetic properties are extrinsic properties, relating to nanocrystallinity of alloys and preferred arrangement of magnetic domains. The excellent soft magnetism is achieved when fine (~ 15 nm diameter) ferromagnetic nanocrystallites are exchange coupled through a surrounding amorphous matrix. In other words, the grain sizes in the order of 10–15 nm lowers the magneto-crystalline anisotropy proportionally, resulting in superior soft magnetic properties [8].

In crystalline $Fe_{1-x}Co_x$ system, the maximum saturation magnetization (M_s) and minimum magnetocrystalline anisotropy are investigated at concentrations of $x=0.3$ and $x=0.5$, respectively [9]. The magnetostriction coefficient (λ_s) is also significant in equiatomic composition of this alloy system. The M_s decreases in amorphous alloy system owing to the addition of necessary non-magnetic glass former typically, Si and B. Accordingly, M_s as well as λ_s decreases with Co addition in $Fe_{80-x}Co_xB_{20}$ system [10], and maximum saturation magnetization occurs in $Fe_{70}Co_{10}B_{20}$ alloy [11]. In Co added FINEMET alloys, Si has a detrimental effect on saturation magnetization due to the formation of $(Fe,Co)_3Si$ phase than that of (Fe,Co) phase in Si-free alloy, causing less localized moment between Fe and Co atoms in former alloy [1]. On the other hand, Co-based amorphous alloys with small additions of Fe reveal nearly zero λ_s, resulting in good soft magnetic behavior. Their application is limited due to the fact that their saturation induction is considerably lower compared to that of Fe-based alloys [12]. The induced anisotropy plays a dominant role for controlling soft magnetism of nanocrystalline materials, which is

* Corresponding author.
E-mail addresses: rajat@nmlindia.org, rajatroy.k@gmail.com (R.K. Roy).

http://dx.doi.org/10.1016/j.jmmm.2016.02.055
0304-8853/

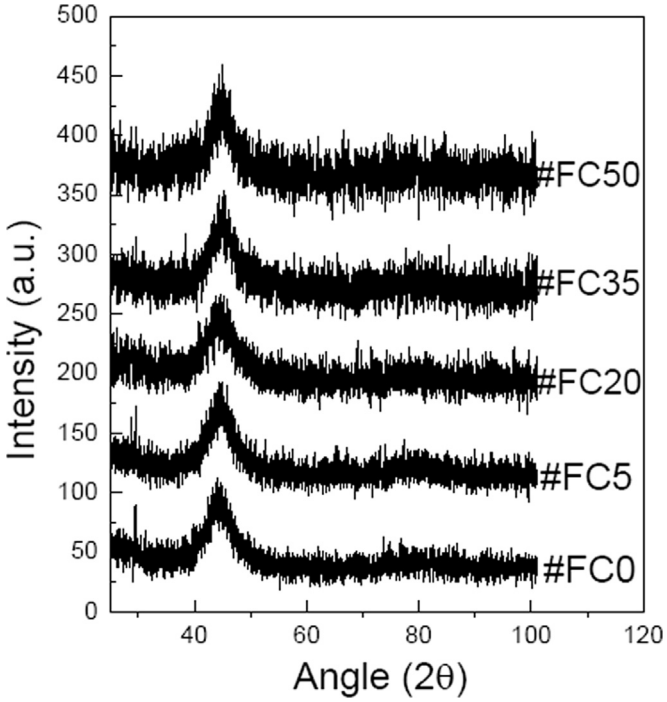

Fig. 1. XRD patterns of as-quenched ribbons.

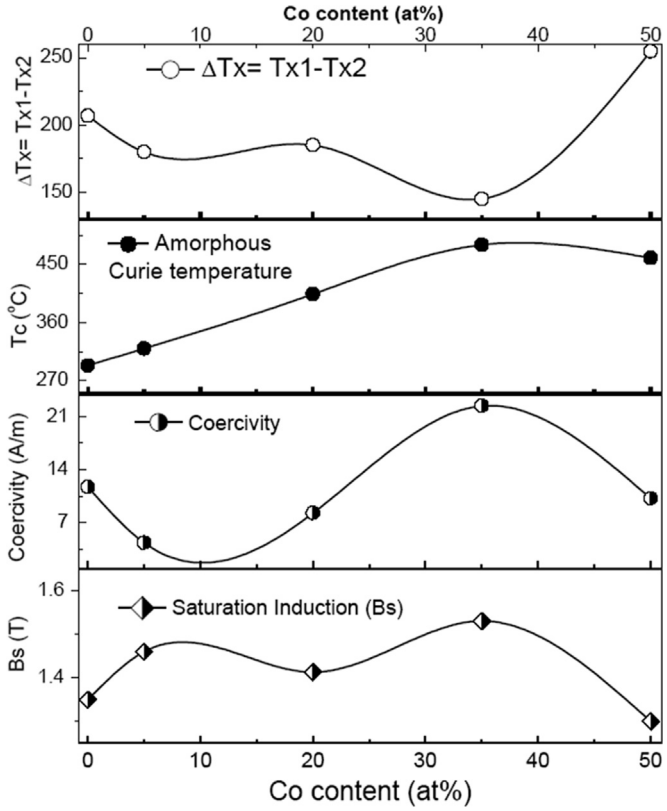

Fig. 2. Co content dependences on thermal and magnetic properties of as-quenched alloys.

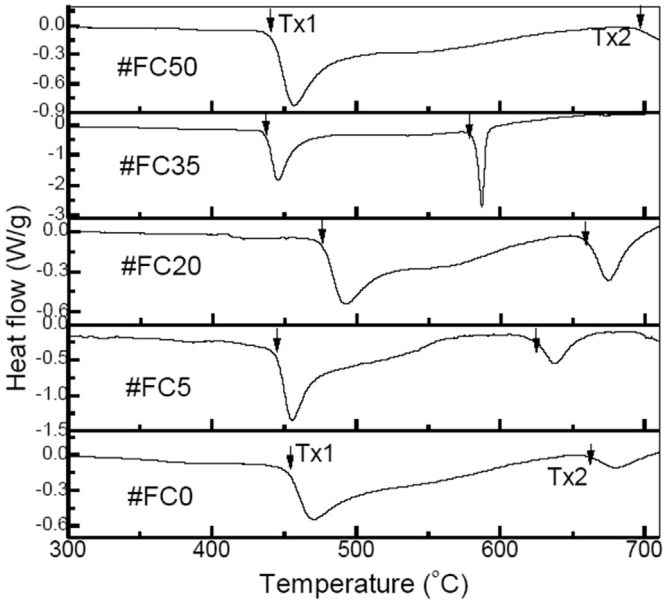

Fig. 3. DSC thermograms of as-quenched alloys.

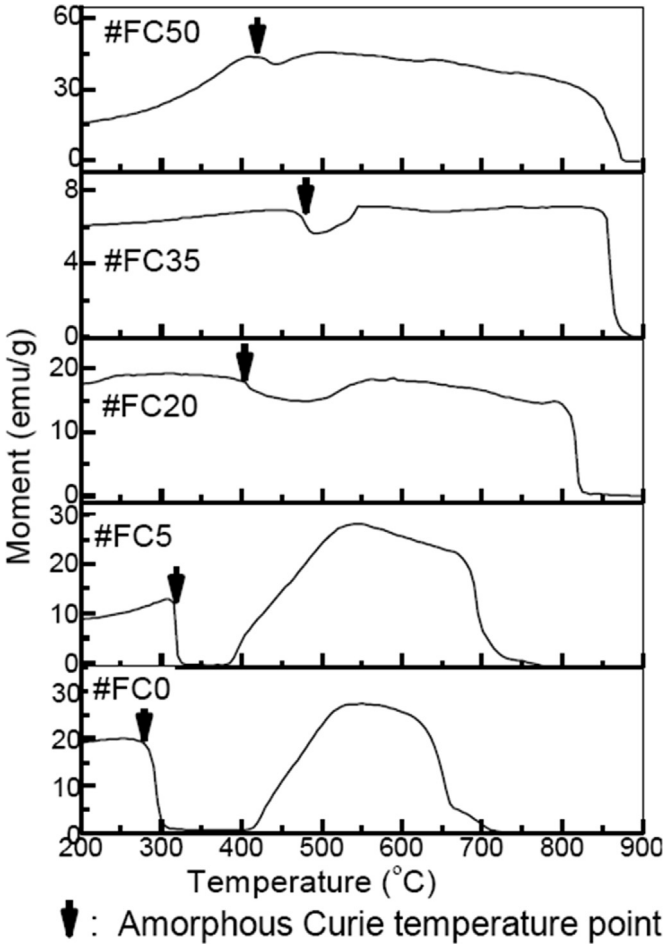

Fig. 4. *M–T* curves of as-quenched alloys, explaining magnetic moment as a function of temperature.

evaluated as strong for amorphous Co based alloy and weak for nanocrystalline Fe based alloy. It improves the soft magnetic properties of latter alloy compared to former alloy [12]. Since nanocrystallites are exchanged coupled through the intergranular amorphous matrix, the increasing of amorphous Curie (T_c) temperature is essentially needed to enhance the soft magnetic properties at elevated temperatures. Therefore, the superior magnetic properties can be achieved with the optimization of alloy compositions and annealing treatment. The focus of this research is to investigate the effect of varying Co content on magnetic properties of a $Fe_{79}Si_{8.5}B_{8.5}Nb_3Cu_1$ amorphous alloy. Our aim

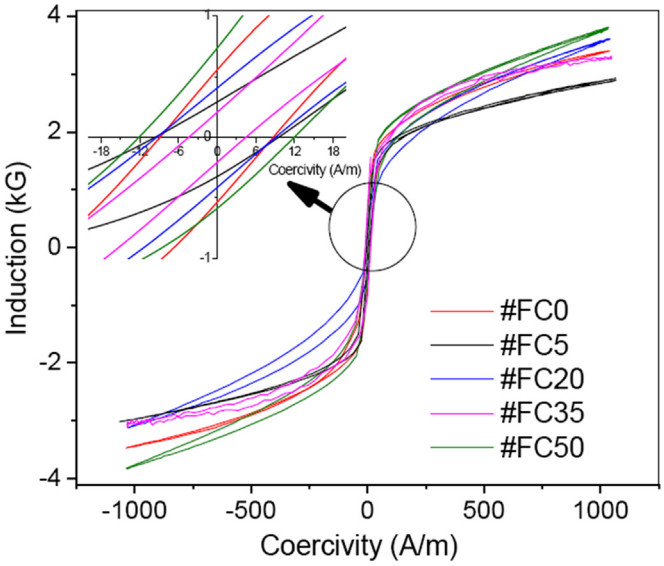

Fig. 5. *B–H* curves of as-quenched alloys (inset showing coercivity variation).

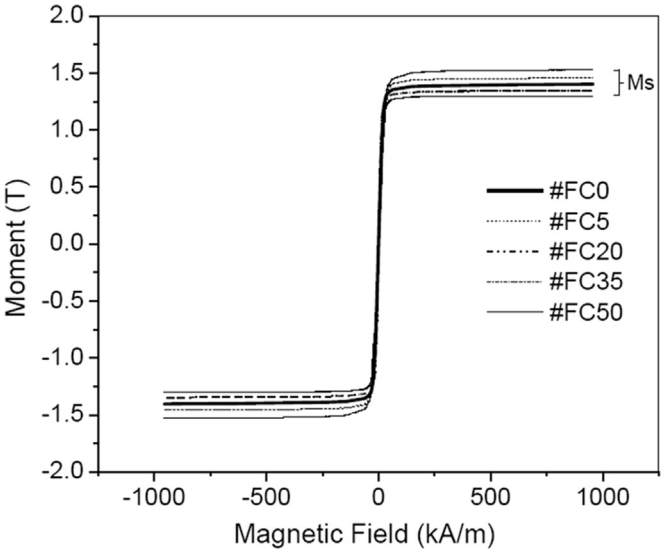

Fig. 6. *M–H* curves of as-quenched alloys.

is to optimize the Co content to obtain the alloys with enhanced thermal stability and good magnetic properties.

2. Experimental procedures

The ribbons (#FC0, #FC5, #FC20, #FC35 and #FC50) of nominal composition $(Fe_{1-x}Co_x)_{79}Si_{8.5}B_{8.5}Nb_3Cu_1$ with varying Co content (x=0, 5, 20, 35 and 50 at%), were prepared by melt spinning method through single copper roller. The as-quenched ribbons were annealed at different temperatures under inert atmosphere, and the effect of nanocrystallinity on magnetic properties has been studied. The thermal behavior of ribbons was examined by a differential scanning calorimetry (DSC) of Perkin Elmer (Diamond DSC) at the heating rate of 20 °C/min. The structure of as-quenched and annealed ribbons was determined by X-ray diffraction (XRD) of Bruker S8 and transmission electron microscopy (TEM) of JEOL (JEM-2000EX-II). The saturation magnetic flux density (B_S) under a maximum applied field of 955 kA/m and the variation of magnetization (M) with temperature were measured by a Lakeshore vibrating sample magnetometer (VSM). The coercivity of

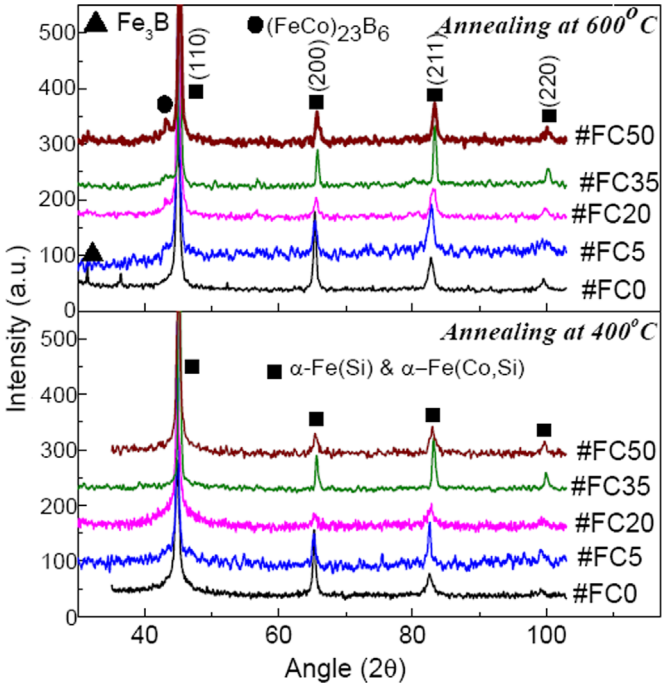

Fig. 7. XRD patterns of alloys annealed at 400 and 600 °C temperatures.

alloys was determined from dc *B–H* curve measured with a *B–H* curve tracer.

3. Results and discussion

The X-ray diffraction spectra of as-quenched ribbons show only a single broad peak, no sharp peak related to crystalline phases is examined at different Co-added alloys (Fig. 1). It indicates the Co addition has no adverse effect on the amorphization of melt spun alloys. Fig. 2 shows the dependency of Co content on thermal and magnetic properties of as-quenched alloys. The crystallization temperatures of alloys are explained by DSC thermograms (Fig. 3). The onsets of primary and secondary crystallization temperatures, T_{x1} and T_{x2}, of alloy #FC0 are 454 and 661 °C, respectively. The addition of 5 (#FC5) and 35 at% Co (#FC35) decrease both T_{x1} and T_{x2}, and 20 at% Co shifts T_{x1} to higher temperature without effecting T_{x2} position. As a consequence, the span (ΔT_x) between the crystallization onsets ($=T_{x2}-T_{x1}$) decreases with increasing Co content up to 35 at%. In contrast, the 50 at% Co incorporation in alloy #FC50 shifts T_{x2} to farthest of 696 °C, resulting in wider ΔT_x which helps easy formation of nanocrystallites in the residual amorphous matrix by annealing between T_{x1} and T_{x2} temperatures. It increases the thermal stability of nanostructured alloys, and enhances high temperature magnetic properties in the ferromagnetic amorphous alloys. The ΔT_x of FeCo based alloys is higher than that of Fe based alloys reported earlier [13–15]. The T_{x1} and T_{x2} correspond to the formation of a ferromagnetic phase at the first stage and some non-magnetic boride phases at the second stage. The ferromagnetic phase is α-Fe for Co-free alloy and α-(Fe, Co) for Co-contained alloys. The ferromagnetic phase formation is also extrapolated in the *M–T* curves of as-quenched alloys (Fig. 4). The magnetic moment of alloys #FC0 and #FC5 becomes zero at amorphous Curie temperature point (T_c) due to ferromagnetic to paramagnetic transition, and it increases again during primary crystallization owing to the ferromagnetic phase formation. For high Co contained alloys (#FC20, #FC35 and #FC50), the magnetic moment decreases a little at amorphous Curie temperature point (T_c), but does not reach zero point due to higher magnetic coupling. The Curie temperature (T_c) has a linear

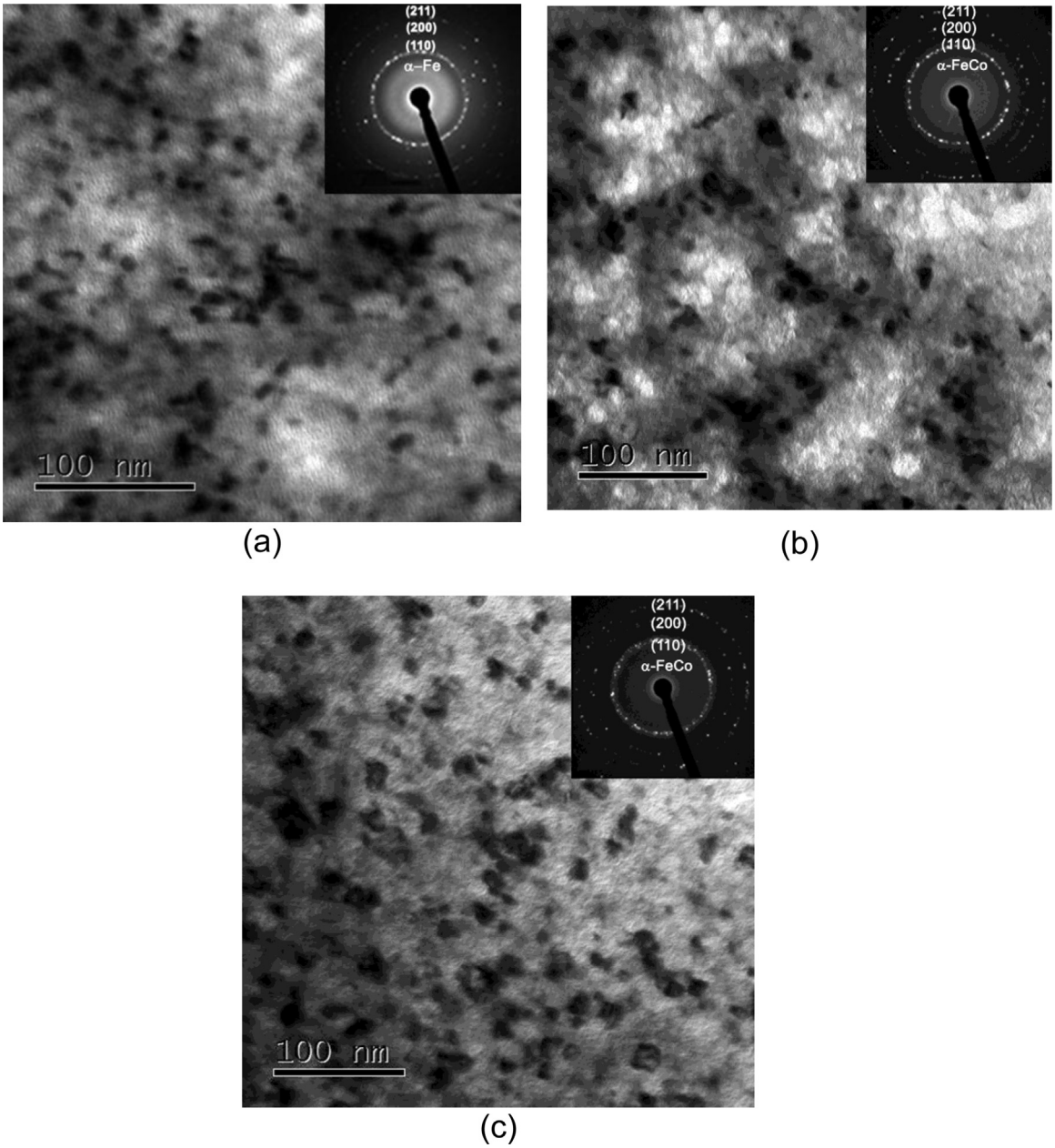

Fig. 8. TEM images and SAED patterns (inset) of annealed (at 600 °C) ribbons of alloys. (a) #FC0 (b) #FC20, (c) #FC50.

relationship to exchange interaction energy (J_{ex}) as per mean field theory, i.e., $T_c \propto J_{ex}$ [16]. As per the Bethe–Slater curve, magnetic exchange interaction energy varies as a function of interatomic spacing, and high temperature magnetic moment of Co based alloys is relatively invariant to disorder than Fe based alloys [17]. Accordingly, in FeCo system, the Curie temperature becomes maximum for the alloys with 35% Co content and decreases for the alloys with higher Co content [9], which is quite comparable for alloys #FC35 and #FC50 for obtaining the highest and lower Curie temperatures, respectively. The coercivity of as-quenched alloys is measured from *B–H* curves (Fig. 5), and it is obtained the alloys #FC0, #FC20 and #FC50 have a nearly same coercivity, while #FC5 and #FC35 generate the minimum and maximum level of coercivity, respectively. The saturation induction (M_s) is determined from *M–H* curves measured through VSM (Fig. 6), and there are maximum and minimum saturation induction achieved for alloys #FC35 and #FC50, respectively. The results can be explained by the random anisotropy model as proposed by Herzer [12], where coercivity (H_c) is directly related to the magnetic anisotropy constant (K) as follows

$$H_c \propto K/M_s \tag{1}$$

where M_s is the saturation induction.

Therefore, the small magnetic anisotropy is equivalent to low coercivity and saturation induction, which is observed in the alloys with an equiatomic ratio of Fe and Co [9]. In other words, the Slater–Pauling curve explains the maximum magnetic moment is achieved within 20–40 at% of Co addition in Fe–Co alloys [16]. As a consequence, the alloy #FC50 with 50 at% Co addition results in the lowering of coercivity and saturation induction. It is noteworthy that Co addition within 5–20 at% results in the lowest coercivity range of 4–8 A/m and moderate saturation induction ranges of 1.41–1.46 T. Hence, the small amount Co content is beneficial for enhanced soft magnetic properties and moderate saturation induction. The Co addition is advantageous not only for enhancing magnetic moment, but also for increasing the Curie temperatures. The higher Curie temperature of amorphous matrix

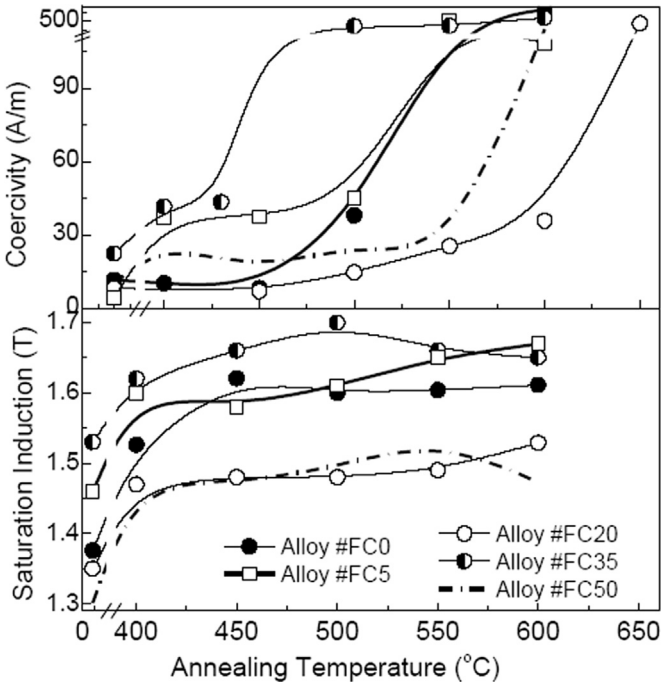

Fig. 9. Saturation induction and coercivity of as-quenched alloys as a function of annealing temperature.

(T_c) also plays a dominant role for controlling soft magnetic properties in nanocomposites at elevated temperatures. It occurs because the intergranular coupling decreases at high measuring temperature near T_c, and the domain structure transforms from a wide pattern to a small and irregular pattern [12]. Accordingly, the higher Curie temperature of amorphous matrix is essentially needed to enhance soft magnetic properties for high temperature magnetic applications. This is discussed later in details.

The structure of alloys is characterized by XRD and TEM, identifying different phases and their morphologies. Fig. 7 represents XRD patterns of alloys annealed at 400 and 600 °C. After annealing at 400 °C, the alloys show the distribution of nanocrystallites, α-Fe and α-FeCo phases in the amorphous matrix of alloy #FC0 and Co-containing other alloys, respectively. The lattice parameter of α-Fe has been found about 0.286 nm, which is lower than that of pure Fe (a_{Fe}=0.2866 nm) [18]. Partitioning of Si with smaller atomic radius into Fe leads to shrinkage in the lattice parameter of nanocrystalline α-Fe phases, resembling the nanocrystalline α-Fe(Si) phase [4]. Similarly, the alloys #C20 and #C50 also evidence the lattice parameter values of 0.2851 and 0.2847 nm, respectively, which are lower compared to pure Fe–Co phases for similar compositions [19,20], indicating the formation of α-Fe(Co,Si) phase. The lowering of lattice parameter signifies more lattice disturbance in nanocrystallites phases with Co addition. It is attributed as the peak broadening along with (110) crystalline peaks in 400 °C annealed samples. Subsequently, the orthorhombic Fe_3B phase formation is observed after annealing at 600 °C, which is similar to the reported results for $(FeCo)_{78}Si_9B_{13}$ alloy [21]. Upon further annealing, the structure is stabilized with the transformation of metastable Fe_3B phase to equilibrium Fe_2B and $(Fe,Co)_{23}B_6$ phases for Fe and FeCo based alloys, respectively [22].

Fig. 8 explains TEM microstructure of the alloys (#FC0, #FC20 and #FC50) annealed at 600 °C. The α-Fe (for #FC0) and α-FeCo (for #FC20 and #FC50) nanocrystallites are homogeneously distributed throughout in the amorphous matrix, which is confirmed by selected area diffraction (SAED) patterns (Fig. 8 insets). The average nanocrystallite size of alloy #FC20 (13 nm) is finer than that of alloys #FC0 (14 nm) and #FC50 (16 nm). A diffuse ring is examined near the center of SAED is presumed the amorphous matrix, which is more prominent in alloy #FC0 and #FC20 (Fig. 8a and b). It indicates a small amount (~20 at%) Co is comparable to Co-free alloy and more significant for the distribution of fine nanocrystallites in the amorphous matrix.

Magnetic properties such as saturation induction and coercivity of as-quenched (AQ) and annealed alloys are explained in Fig. 9. The saturation induction as a function of Co content is discussed in Fig. 2. Upon annealing, the saturation induction of annealed Co-added alloys (#FC20 and #FC50) is lower than that of annealed Co-free alloy. However, the saturation induction variation of #FC5 and #FC35 is higher compared to #FC0. This trend is lower in amorphous Fe–Co alloys than in crystalline alloys owing to the presence of glass forming metalloid elements B and Si [10]. It is more significant in high Si containing FINEMET alloys with Co addition, wherein saturation magnetization continuously deteriorates with increasing annealing temperature [21]. However, we examined here saturation magnetization of amorphous alloys increases with annealing temperature. This is attributed to the high FeCo and low Si contents in these alloys, resulting in an increased magnetic moment and a reduced effect of α-Fe(Co,Si) phase. The increased Curie temperatures (T_c) of Co added alloys have a good agreement with it. Moreover, the moderate Co addition also has an immense effect on the improvement of soft magnetic properties. Although the coercivity of Co-free and Co-added alloys varies within a nominal range (8–22 A/m) for as-quenched condition, however, it varies within a wide span between 19–522 A/m after annealing at 550 °C. Above all, a small amount Co addition (alloy #FC20) plays a dominant role for improving soft magnetic properties compared to alloys #FC5, #FC35 and #FC50. It is attributed to the compositional variation of amorphous matrix upon annealing treatment of materials. The nanocrystallization process of FeCo based amorphous alloy is a consequence of α-FeCo crystallite formation and the enrichment of B, Nb and Co/(Fe+Co) ratio in the amorphous matrix. Although the nanocrystallites are enriched with Fe relative to the matrix [22], the diffusion of Si into α-Fe and consequent growth of nanocrystallites is impeded by Nb layer existing at the interface of nanocrystallites and amorphous matrix [23]. The Co/(Fe+Co) ratio in amorphous matrix plays a key role for controlling nanocrystallization. Accordingly, the temperature dependence of soft magnetic properties varies with Co addition, improving coercivity with the presence of small amount Co. The low content of Co in combination with dominant presence of Fe in the matrix, improved the stability of amorphous matrix by enhancing the intergranular exchange interaction through amorphous matrix leading to improvement in soft magnetic property (coercivity). In higher Co containing alloys (#FC35 and #FC50), the excess Co atoms in amorphous matrix cause structural fluctuations which give rise to fluctuation in the exchange interactions. It reduces magnetic coupling, resulting in the deterioration in soft magnetic properties at elevated temperatures approaching to Curie temperatures of those alloys [12].

In nanocrystalline materials, magnetic properties are controlled by the exchange of magnetic coupling between bcc nanocrystallites through intergranular amorphous matrix [24]. Therefore, the Curie temperature of amorphous matrix (T_c) is prevalent for affecting temperature dependent soft magnetism. The soft magnetic properties of FINEMET alloys degrade rapidly at temperature near T_c owing to the reduction of intergranular magnetic coupling and the transformation of wide domain to small and irregular domain [25,26]. This phenomenon is true for Co free alloy #FC0. However, the Co addition, such as in alloys #FC20 and #FC50, modifies the nanocrystalline phases as well as intergranular amorphous matrix, causing an increased magnetic coupling above the Curie point of amorphous matrix (T_c), therefore, the soft magnetic properties are improved above T_c.

4. Conclusions

The ribbons of nominal composition $(Fe_{1-x}Co_x)_{79}Si_{8.5}B_{8.5}Nb_3Cu_1$ show no adverse effect of amorphization with Co addition. The higher Co content also increases the Curie temperatures as well as thermal stability. A small amount Co (~20 at%) results in coercivity of 35 A/m after annealing at 600 °C, which is about 10–25 times lower than that of the alloys with equiatomic Fe:Co ratio and Co-free. The nanocrystallites size also becomes finer in former alloy than latter compositions. Simultaneously, the alloy with 20% Co addition shows saturation induction above 1.5 T after annealing at 600 °C.

Acknowledgment

The authors acknowledge to in-house project (OLP210) of CSIR-NML for financial support and Director, CSIR-NML, for giving permission for this publication.

References

[1] M.A. Willard, M. Daniil, K.E. Kniping, Nanocrystalline soft magnetic materials at high temperatures: a perspective, Scr. Mater. 67 (2012) 554–559.
[2] Y. Yoshizawa, S. Oguma, K. Yamauchi, New Fe-based soft magnetic alloys composed of ultrafine grain structure, J. Appl. Phys. 64 (1988) 6044–6046.
[3] Y. Yoshizawa, K. Yamauchi, T. Yamane, H. Sugihara, Common-mode choke cores using the new Fe-based alloys composed of ultrafine grain structure, J. Appl. Phys. 64 (1988) 6047–6049.
[4] A.K. Panda, B. Ravikumar, S. Basu, A. Mitra, Crystallization and soft magnetic properties of rapidly solidified $Fe_{73.5}Nb3Cu1Si_{22.5-x}B_x$ ($x=5$, 9, 10, 11.25, 19) alloys, J. Magn. Magn. Mater. 260 (2003) 70–77.
[5] A. Kojima, H. Horikiri, Y. Kamamura, A. Makino, A. Inoue, T. Matsumoto, Production of nanocrystalline b.c.c. Fe-Nb-B bulk alloys by warm extrusion and their magnetic properties, Mater. Sci. Eng. A 179 (1994) 511–515.
[6] M.A. Willard, M.Q. Huang, D.E. Laughlin, M.E. McHenry, J.O. Cross, V.G. Harris, C. Frascetti, Magnetic properties of HITPERM $(Fe,Co)_{88}Zr_7B_4Cu_1$ magnets, J. Appl. Phys. 85 (1999) 4421.
[7] M.A. Willard, D.E. Laughlin, M.E. McHenry, D. Thomas, K. Sickafus, J.O. Cross, et al., Structure and magnetic properties of $(Fe0.5Co_{0.5})_{88}Zr_7B_4Cu_1$ nanocrystalline alloys, J. Appl. Phys. 84 (1998) 6773.
[8] G. Herzer, in: K.H.J. Buschow (Ed.), Handbook of Magnetic Materials, 10, Elsevier Science, United States, 1997, pp. 415–462.
[9] F. Pfeifer, C. Radeloff, Soft magnetic Ni–Fe and Co–Fe alloys - some physical and metallurgical aspects, J. Magn. Magn. Mater. 19 (1980) 190–207.
[10] R. Boll, H.R. Hilzinger, H. Warlimont, in: R. Hasegawa (Ed.), The Magnetic, Chemical and Structural Properties of Glassy Metallic Alloys, CRC Press, Boca Raton, FL, 1983.
[11] R.C. O'Handley, R. Hasegawa, R. Ray, C.P. Chou, Ferromagnetic properties of some new metallic glasses, Appl. Phys. Lett. 29 (6) (1976) 330–332.
[12] G. Herzer, Modern soft magnets: amorphous and nanocrystalline materials, Acta Mater. 61 (2013) 718–734.
[13] A. Urata, H. Matsumoto, S. Yoshida, A. Makino, Fe–B–P–Cu nanocrystalline soft magnetic alloys with high B_s, J. Alloy. Compd. 509 (2011) S431–S433.
[14] A. Makino, H. Men, K. Yubuta, T. Kubota, Soft magnetic FeSiBPCu hetero-amorphous alloys with high Fe content, J. Appl. Phys. 105 (2009) 013922.
[15] T. Kubota, A. Makino, A. Inoue, Low core loss of $Fe_{85}Si_2B_8P_4Cu_1$ nanocrystalline alloys with high B_s and B_{800}, J. Alloy. Compd. 509 (2011) S416–S419.
[16] M.E. McHenry, M.A. Willard, D.E. Laughlin, Amorphous and nanocrystalline materials for applications as soft magnetic, Prog. Mater. Sci. 44 (1999) 291–433.
[17] A. Gallagher, M.A. Willard, V.N. Zabenkin, D.E. Laughlin, M.E. McHenry, Distributed Exchange Interactions and Temperature Dependent Magnetization in Amorphous $Fe_{88-x}Co_xZr_7B_4Cu_1$ Alloys, J. Appl. Phys. 85 (1999) 5130–5132.
[18] B.D. Cullity, Elements of X-ray Diffraction, 1978, p. 102.
[19] W.C. Ellis, E.S. Greiner, Relations in the solid state of the iron–cobalt system, Trans. ASM 29 (1941) 415–434.
[20] I. Ohnuma, H. Enoki, O. Ikeda, R. Kainuma, H. Ohtani, B. Sundman, K. Ishida, Phase equilibria in the Fe–Co binary system, Acta Mater. 50 (2002) 379–393.
[21] A. Kolano-Burian, J. Ferenc, T. Kulik, Structure and magnetic properties of high temperature nanocrystalline Fe–Co–Cu–Nb–Si–B alloys, Mater. Sci. Eng. A 375–377 (2004) 1078–1082.
[22] Y. Zhang, J.S. Blázquez, A. Conde, P.J. Warren, A. Cerezo, Partitioning of Co during crystallisation of Fe–Co–Nb–B(–Cu) amorphous alloys, Mater. Sci. Eng. A 353 (2003) 158–163.
[23] R.K. Roy, S.J. Kernion, S. Shen, M.E. McHenry, Crystallization behavior and high temperature magnetic phase transitions of Nb-substituted FeCoSiBCu nanocomposites, Appl. Phys. Lett. 99 (2011) 192506.
[24] G. Herzer, Soft magnetic nanocrystalline materials, Scr. Mater. 33 (1995) 1741 1756.
[25] R. Schäfer, A. Hubert, G. Herzer, Domain observation on nanocrystalline material, J. Appl. Phys. 69 (1991) 5325.
[26] S. Flohrer, R. Schäfer, Polak Ch., G. Herzer, Interplay of uniform and random anisotropy in nanocrystalline soft magnetic alloys, Acta Mater. 53 (2005) 2937–2942.